

Splicing factor Rbm10 facilitates heterochromatin assembly in fission yeast

Martina Weigt^{1,†}, Qingsong Gao^{1,†}, Hyoju Ban^{2,†}, Haijin He², Guido Mastrobuoni³ and
Stefan Kempa³, Wei Chen^{1,4,5,*}, and Fei Li^{2,*}

¹Laboratory for Functional Genomics and Systems Biology, Berlin Institute for Medical Systems Biology, Max-Delbrück-Center for Molecular Medicine, Berlin 13125, Germany.

²Department of Biology, New York University, New York, NY 10003-6688, USA

³Integrative Metabolomics and Proteomics, Berlin Institute of Medical Systems Biology, Max-Delbrueck Center for Molecular Medicine, Berlin 13125, Germany.

⁴Department of Biology, Southern University of Science and Technology, Shenzhen, Guangdong, China

⁵Medi-X Institute, SUSTech Academy for Advanced Interdisciplinary Studies, Southern University of Science and Technology, Shenzhen, Guangdong, China

*To whom correspondence should be addressed. Tel: +1 212 998 3746; Fax: +1 212 995-4015; Email: fl43@nyu.edu

Correspondence may also be addressed to Wei Chen. Email: chenw@sustc.edu.cn

†These authors contributed equally to this work as first authors.

Keywords: epigenetics; splicing factor; *Schizosaccharomyces pombe*; histone deacetylase; H3K9 methylation

ABSTRACT

Splicing factors have recently been shown to be involved in heterochromatin formation, but their role in controlling heterochromatin structure and function remains poorly understood. In this study, we identified a fission yeast homologue of human splicing factor RBM10, which has been linked to TARP syndrome. Overexpression of Rbm10 in fission yeast leads to strong global intron retention. Rbm10 also interacts with splicing factors in a pattern resembling that of human RBM10, suggesting that the function of Rbm10 as a splicing regulator is conserved. Surprisingly, our deep-sequencing data showed that deletion of Rbm10 caused only minor effect on genome-wide gene expression and splicing. However, the mutant displays severe heterochromatin defects. Further analyses confirmed that the heterochromatin defects in the mutant did not result from mis-splicing of heterochromatin factors. Our proteomic data revealed that Rbm10 associates with the histone deacetylase Clr6 complex and chromatin remodeling complexes known to be essential for heterochromatin silencing. Our work together with previous findings further suggests that different splicing subunits may play distinct roles in heterochromatin regulation.

INTRODUCTION

In eukaryotic cells, DNA and histones are organized into the highly-ordered chromatin structure. Chromatin forms two distinct domains, euchromatin and heterochromatin. Euchromatin is less condensed and associated with actively transcribed genes, whereas heterochromatin is tightly coiled and transcriptionally inactive. Heterochromatin usually consists of highly repetitive sequences, which are commonly found around pericentromeres and telomeres. Heterochromatin plays essential roles in gene expression, chromosome segregation and genome stability (1-3).

The pattern of histone modifications in heterochromatin contributes to the organization of the chromatin domain. Heterochromatin is characterized by hypoacetylation of histone lysines and methylation of histone H3 on lysine 9 (H3K9me) (1,3). Histone deacetylases (HDACs) are responsible for hypoacetylation in heterochromatin, while H3K9me is catalyzed by the histone methyltransferase SUV39, an enzyme conserved from fission yeast to humans. H3K9me serves as a binding site for heterochromatin protein 1 (HP1), which recruits additional factors to mediate heterochromatin assembly (1,3). Small interfering RNAs (siRNAs) generated by RNA interference pathway have been shown to be important for heterochromatin structure and function in a variety of organisms (1). However, the mechanisms underlying the heterochromatin formation remain poorly understood

The fission yeast *Schizosaccharomyces pombe* has emerged as an excellent model organism for understanding heterochromatin formation. It harbors three constitutive heterochromatic regions: the pericentromere, telomere and mating type region. These regions are enriched with H3K9me, which is recognized by the human HP1 homolog, Swi6. H3K9me in fission yeast heterochromatin is regulated by the multi-subunit CLRC complex, which contains Clr4,

the H3K9 methyltransferase, Rik1, Dos1/Raf1, Dos2/Raf2, Cul4 and Lid2, a H3K4 demethylase (4-9). H3K9 methylation in heterochromatin also requires RNAi.

Heterochromatin is transcribed during S phase of the cell cycle (10,11). The heterochromatin transcripts are subsequently processed into siRNAs by Ago1, the RDRC complex and Dicer. The siRNAs are loaded into RITS complex (Ago1, Chp1 and Tas3), which in turn guides the CLRC complex to heterochromatin regions (1,12,13) to mediate H3K9me. The DNA Pol II epsilon subunit, Cdc20, also contributes to the recruitment of ClrC complex during the S phase (14-16).

Like other eukaryotes, histones in fission yeast heterochromatin are hypoacetylated. Fission yeast contains all three subtypes of histone deacetylases (HDACs): Class I, Class II and Class III. Clr6, a Class I HDAC, is a homolog of mammalian HDAC1 and HDAC2, and deacetylate multiple lysine residues on histone H3 and H4. Clr3 is a Class II HDAC, responsible for H3K14 deacetylation (17,18). Sir2 is a conserved member of the Sirtuin family of Class III HDACs that uses NAD^+ as a cofactor (19,20). All of these HDAC contributes to heterochromatin silencing in fission yeast (17).

Recently, splicing factors have been linked to heterochromatin formation in fission yeast. But the mechanisms for how these splicing factors participate in heterochromatin formation remains unclear. A prevailing model proposes that splicing factors, independently from splicing, directly interacts with RNAi components to mediate the recruitments of the CLRC complex to heterochromatic regions (21). Another study suggests that transcripts derived from pericentromeric repeats contain introns, and splicing factors may mediate the splicing of the intron of the heterochromatin transcripts, which in turn influences siRNA generation (22). A more recent study by Kallegren, et al. suggested that splicing factors may contribute to

heterochromatin assembly indirectly by regulating the proper splicing of heterochromatin factors (23).

RBM10 has been recently characterized as a new member of splicing factors, and associated with lung cancer and congenital disorders, such as the TARP syndrome and XLMR (24-27). RBM10 contains five distinct domains, including two RNA recognition motifs (RRM), two zinc fingers and one G patch motif. Splicing involves an ordered, stepwise rearrangement of protein and RNA content in spliceosome. An early step in spliceosome assembly is the formation of the prespliceosome (complex A). The prespliceosome rearranges to the precatalytic spliceosome (complex B), which subsequently gives rise to the activated spliceosome (complex B*). Complex B* carries out the first catalytic step of splicing, generating complex C, which in turn carries out the second catalytic step (28). It has been shown that RBM10 is associated with prespliceosome (complex A) and activated spliceosome (complex B*) in human cells (29-33). The human RBM10 has been shown to regulate exon skipping by repressing the splicing of introns (24). In addition to its role in splicing, human RBM10 was also found to be part of histone H2A deubiquitinase complex (34), suggesting a role in linking splicing and chromatin regulation.

In this study, we identified a fission yeast homologue of RBM10, which was named *rbm10*⁺. Overexpression of Rbm10 in fission yeast results in strong growth defects and global intron retention. We found that Rbm10 also associated with splicing factors in a pattern similar to that of human RBM10. These results suggest that the role of Rbm10 as a splicing factor is conserved. However, our RNA deep sequencing (RNA-seq) analysis revealed that surprisingly deletion of *rbm10*⁺ has little effect on splicing and gene expression. But we found that heterochromatin formation is severely impaired in the mutant. Our TAP

purification combined with mass spectrometry analysis demonstrated that Rbm10 interacts with the conserved histone deacetylase Clr6 complex and the chromatin remodelers instead of RNAi components. The present and previous studies together suggest that different splicing subunits may control heterochromatin formation in separate manners. We speculate that specific environmental cues may induce higher expression of *rbm10*⁺, which in turn impacts on gene expression through altering RNA splicing patterns.

MATERIALS AND METHODS

Fission yeast strains and genetic analysis

*rbm10*Δ, *rbm10-GFP* and *FLAG-HA-rbm10* strains were constructed via a PCR-based homologous recombination and verified by PCRs. pREP1-*FLAG-HA-rbm10* and pREP1-*pku70* were constructed by inserting their respective cDNAs into NdeI/BamHI or Sall/SmaI sites in the plasmid. pDUAL constructs were derived from the *S. pombe* ORFeome library (Riken Bioresource Center). Genetic crosses were conducted following standard protocols (35). For silencing assays, a series of 10-fold dilutions with a starting concentration of 2×10⁷ cells/ml were spotted on the designated media and incubated at 30°C for 2-3 days.

RNA Sequencing

RNA sequencing was performed as described (24). Briefly, poly (A) RNA was prepared from total RNA by two rounds of oligo (dT)₂₅ Dynabeads (Invitrogen) purification. Following fragmentation at 94°C for 3.5 min, the RNA was converted to first strand cDNA using random hexmer primer and Superscript II (Invitrogen), followed by second strand cDNA synthesis with *Escherichia coli* DNA pol I (Invitrogen) and RNase H (Invitrogen). The barcoded sequencing library was prepared and sequenced on Illumina HiSeq for 1 × 100 cycles following the standard protocol.

RNA-Seq data analysis

RNA-seq reads that pass the Illumina filter were aligned to the *S. pombe* genome reference sequences (version: ASM294v2) using TopHat with default mapping parameters (version 2.0.8) (36). The read count for each exon-exon and/or exon-intron junction as well as each gene was produced by custom Perl script. DESeq package was used to identify the differentially expressed genes between *rbm10* Δ cells and WT (37). Adjusted p.value < 0.05 was used as the threshold for determining significance. Fisher's exact test was used to compare the splicing pattern of each exon (for exon skipping) or each intron (for intron retention) between *rbm10* Δ cells and WT. Adjusted p.value < 0.05 and $|\Delta\text{PSI}|$ (or $|\text{PIR}|$) > 10% was used as the threshold for determining significant splicing difference.

ChIP

ChIP was performed by as previously described (14). Briefly, 50 ml of a log-phase yeast culture was cross-linked by adding 37% formaldehyde for 30 min. Cells were collected and sonicated by an Ultrasonic Processor. 1 μl of H3K9me antibody (Abcam ab1220) was used for immunoprecipitation. Immunoprecipitated DNA was purified using a PCR clean up column (Qiagen), and analyzed by PCR using primers listed in Supplementary Table S8. The experiments were replicated in two or three independent biological repeats.

RT-PCR

500 ng starting material of total RNA was used per reaction. First strand synthesis was performed with Random Primer and Superscript II RT (Invitrogen) at 25°C for 10 min, then 42°C for 50 min and 70°C for 15 min. For the subsequent PCR 1 μl from the reverse transcriptase reaction was used. Oligos used are listed in Supplementary Table S8.

TAP-tag purification and mass spectrometry analysis

Cells carrying pREP1-*FLAG-HA-rbm10* was induced for 24h in minimal media without thiamine. Cells were collected and lysed in lysis buffer with 4 μ l/ml Benzonase by bead beating. Protein G beads coated with anti-FLAG-antibody were added to the cell lysate, and incubated for 1 hour at 4°C on rotation. After washing, the sample was eluted using 3 \times FLAG peptide (Sigma). The eluate was subsequently incubated with uMACS HA magnetic beads on ice for 30 min with occasionally mixing. The eluate with the beads was loaded on a uMACS column, and washed three times with wash buffer I and twice with wash buffer II. To prepare the sample for MS, proteins on the column were predigested by adding 25 μ l 2M urea in 100 mM Tris-HCl pH 7.5, 1 mM DTT and 150 ng Trypsin for 30 min at RT. The sample was eluted by adding 2 times 50 μ l 2M urea in 100 mM Tris-HCl, pH 7.5 and 5 mM iodoacetamide. The sample was digested overnight at RT. 1 μ l trifluoroacetic acid was added to stop the digestion. Mass spectrometry analysis was conducted in the Proteomics platform at Berlin Institute for Medical Systems Biology.

Co-immunoprecipitation

Cells used contain the pREP1-*FLAG-HA-rbm10*, and the pDUAL plasmid carrying a FLAG-His-tagged prey gene under *nmt1* promoter. Cell expressing the FLAG-His-tagged prey gene alone was used for control. Low-level expression was induced by the addition of 0.01 mM thiamine in media for 24h. Cells were collected and resuspended in 100 μ l of 1 \times lysis buffer with protease inhibitors prior to lysis by bead beating. Following treatment with Benzonase, 50 μ l of uMACS HA magnetic beads was added to the lysate and incubated on ice for 30 min with occasionally mixing. Lysate-bead mixture was loaded onto a uMACS column followed by washing with ice-cold lysis buffer. The sample was eluted and analyzed by Western

Blotting. Antibodies used include an anti-FLAG antibody (Sigma) and an anti-His antibody (MBL).

RESULTS

Human splicing factor RBM10 is conserved in *S. pombe*

Via homolog search, we identified SPAC57A7.13, an uncharacterized protein, as the homolog of human RBM10 in *S. pombe*. We hereafter named it Rbm10. The human RBM10 and its *S. pombe* homolog share an amino acid identity of 26% (Supplementary Figure S1). Despite relatively short length of Rbm10 in fission yeast, all five domains are well conserved, namely, two zinc-finger domains, two RRM-motifs and a G-patch domain (Figure 1A). Majority of Zinc-finger domains functions as interaction modules that bind DNA, RNA or proteins (38,39), whereas RRM motifs and the G-patch domain usually associate with RNA (40). To determine the cellular distribution of Rbm10, we constructed the GFP-tagged *rbm10*⁺ under its native promoter and replaced the endogenous *rbm10*⁺. We found that, similar to human RBM10, Rbm10-GFP is enriched in the nucleus (Figure 1B).

Overexpression of Rbm10 leads to massive intron retention

To characterize the function of Rbm10 in fission yeast, we constructed *rbm10*⁺ under the strong, inducible *nmt1* promoter and overexpress it in wild-type cells. The *nmt1* promoter is induced in the absence of thiamine. We found that overexpression of Rbm10 in wild type results in slow growth (Figure 2A). In addition to the strong growth defects, cells overexpressing Rbm10 display aberrant cell shapes. They are often massively elongated or branched in to Y-like shapes. The nuclei in these cells also appear to be abnormal. Multiple fragmented nuclei were frequently observed (Figure 2B). Given that *rbm10*Δ showed only a mild phenotype, we were surprised to find the observed toxicity resulting from

overexpression of Rbm10. To gain insight into the molecular nature of Rbm10 overexpression, we performed unbiased genome-wide RNA-seq using cells overexpressing Rbm10. Cells overexpressing for 20 hours were used to minimize secondary effects. We detected massive changes in intron retention from the RNA-seq data (Figure 2C and Supplementary Table S1 and S2). 2263 introns showed increased retention, whereas 6 introns have decreased retention. These data demonstrated that Rbm10's function as a splicing regulator is conserved in fission yeast, which can be observed at least under overexpression condition.

Deletion of *rbm10*⁺ induces minor changes in gene expression and intron retention

To further understand the role of Rbm10, we constructed a deletion strain, *rbm10*Δ, in which the complete gene was replaced with a kanamycin selection cassette via homologous recombination. *rbm10*Δ cells are viable and do not show obvious growth defects, indicating that Rbm10 is not essential for viability.

To investigate how Rbm10 affects gene expression and splicing, we performed genome-wide RNA-seq in the *rbm10*Δ mutant. We reproducibly found that out of 6748 genes, the expressions of 292 genes in *rbm10*Δ cells were increased compared to wild type, whereas the gene expressions of 99 genes were reduced in the mutant (Figure 3A and Supplementary Table S3 and S4). However, the fold-changes of these gene expressions were very modest, with only 21 (0.3%) genes whose expression altered more than 2 fold. Our RNA-seq also allowed us to analyze the effect of *rbm10*Δ mutant on the intron splicing. Out of 5357 expressed introns, we detected 38 intron retention events in *rbm10*Δ mutant (Percent Intron Retained difference (Δ PIR) > 10%, Figure 3B and Supplementary Table S5). We also found that 7 intron splicing have been enhanced (Δ PIR < 10%, Figure 3B and Supplementary Table

S6). Again, the majority of these changes were affected to a modest level. Previous studies have shown that alternative splicing exists in fission yeast, although not very common (41). Given that human RBM10 is involved in alternative exon usage (42), we also examined alternative exon usage in *rbm10* Δ mutant. However, our results show that no case with significant difference between WT and *rbm10* Δ mutant can be detected (Figure 3C). Taken together, our results show that deletion of Rbm10 has minor effect on gene expression and splicing.

Wang et al. proposed that human RBM10 promotes exon skipping via binding in the vicinity of splice sides, resulting in delaying their splicing choice; thus, these exons with relatively weaker splice side become more excluded during alternative splicing (24). However, alternative splicing is a very rare event in fission yeast (41). It is likely that a delay in splicing resulting from Rbm10 splicing activity does not manifest in alternative splicing, but rather in intron retention. Our data showing a dramatic increase in intron retention in *S. pombe* cells overexpressing Rbm10 is consistent with this idea.

Deletion of *rbm10*⁺ leads to impaired heterochromatin silencing

Splicing factors have been implicated in heterochromatin assembly. We next characterized how Rbm10 affects heterochromatin status. Fission yeast harbors three constitutive heterochromatic regions, namely pericentromeres, telomeres and the mating type locus. To analyze pericentromeric silencing in *rbm10* Δ mutant, a wild type (WT) strain carrying a *ura4*⁺ reporter integrated in the pericentromeric outer repeat (*otr*) was crossed with the mutant. The resulting *rbm10* Δ cells with *ura4*⁺ reporter at *otr* region were analyzed by growth assays in the medium without uracil. The *rbm10* Δ cells grow significantly slower than WT (Figure 4A), indicating that the pericentromeric silencing in the mutant is disrupted. The

strains were further analyzed in the media containing 5-fluoro-orotic acid (FOA), which is toxic to cells expressing uracil. WT cells exhibit strong silencing in *otr* region, as indicated by their robust growth in the FOA media. The slow growth of the *rbm10* Δ cells in the FOA media (Figure 4A) confirmed that the silencing at pericentromeric heterochromatin in *rbm10* Δ mutant is lost.

We also examined the heterochromatin silencing in telomere and mating type locus in *rbm10* Δ using *his3*⁺ and *ura4*⁺ reporters inserted to these regions, respectively. Our growth assays using minimum media without histidine demonstrated that silencing in telomere is strongly lost in *rbm10* Δ cells (Figure 4B). However, *rbm10* Δ cells with *ura4*⁺ in mating type locus did not show major growth deficiency relative to WT in minimum media without uracil and the counter-selective FOA medium (Figure 4C), indicating that the heterochromatin silencing in this region is not significantly affected by deletion of *rbm10*⁺. This different effect between centromere and mating type heterochromatin in *rbm10* Δ is likely due to the redundant pathways involved in heterochromatin formation in mating-type locus.

We next analyzed H3K9me in centromeres and telomeres using ChIP. We observed that H3K9me level is reduced to approximately 50% of WT at both peri-centromeres and telomeres in *rbm10* Δ (Figure 4D). The loss of H3K9me at peri-centromeres and telomeres is consistent with our growth assays, indicating that heterochromatin silencing is impaired in these regions in *rbm10* Δ .

Defects in silencing are not caused by mis-splicing of heterochromatin factors

It has been shown that mutants of splicing factors, such as Cwf14, can induce mis-splicing of mRNA transcripts from heterochromatin factors, including Ago1, which in turn results in

heterochromatin defect (23). The minor differences in *rbm10* Δ in intron retention as shown by transcriptome profiling from the mutant suggests that a secondary effect by *rbm10* Δ via the splicing of heterochromatin factors is unlikely to be the primary cause for heterochromatin defects. A closer look at the mis-spliced transcripts in *rbm10* Δ , however, revealed one factor involved in chromatin organization, *pku70*⁺. *pku70*⁺ is a subunit of telomeric Ku complex important for telomere structure and function. We found that the splicing of several introns of *pku70*⁺ is mildly affected in *rbm10* Δ cells. To confirm this, we performed RT-PCRs with primers designed to analyze the splicing of individual introns, and the results were quantified with Bioanalyzer. We found that each group showed only about 5-10% increase in unspliced transcripts in *rbm10* Δ relative to WT, consistent with the minor defect in *pku70* splicing observed in the strain (Figure 5A and B). Nevertheless, it has been shown that Pku70 is not essential for heterochromatin silencing (43). Consistent with this, we found that silencing defects at the heterochromatin region cannot be rescued by the expression of the wild-type *pku70*⁺ (Figure 5C). From these observations, we conclude that splicing deficiencies are not the major cause for the heterochromatin defects in *rbm10* Δ mutant.

Rbm10 interacts with Clr6, chromatin remodeling complexes and transcription factors

To gain more insight into the function of Rbm10, we determined to identify its interacting proteins using the Tandem Affinity Purification (TAP) method. For this, we constructed a TAP tag with a combination of FLAG and HA tags at the N-terminus of *rbm10*⁺ at its endogenous locus. FLAG-HA-Rbm10 is fully functional, as it does not cause any silencing defects in the pericentromeric *otr* region (Figure 6A). However, we observed that the expression level of endogenous FLAG-HA-Rbm10 is extremely low (Data not shown). We thus constructed FLAG-HA-Rbm10 under the *nmt1* promoter, and overexpressed FLAG-HA-

Rbm10 for TAP tag purification. We collected cells within 24 hours of induction in order to minimize the potential secondary effects. We performed a two-step affinity purification of FLAG-HA-Rbm10 and subjected the sample to mass spectrometry (MS) analysis (Figure 6B). From three independent affinity purifications, we obtained 853 interacting proteins (Figure 6C and Supplementary Table S7) found in all replicates but being absent from control purifications. These proteins included factors involved in heterochromatin silencing, chromatin remodeling, and RNA processing, and transcription (Figure 6D and 7A). GO Term analysis with PANTHER further revealed an overrepresentation of RNA metabolic process ($p=9.75 \times 10^{-5}$), chromatin organization ($p=2.2 \times 10^{-16}$) and DNA-dependent transcription ($p=1.06 \times 10^{-2}$).

Clr6 HDAC complexes are important for heterochromatin silencing, and fall in two main classes I and II in fission yeast (18). Five members from the HDAC Clr6 I complex and also Alp13 from the Clr6 II complex can be found to be associated with Rbm10 (Figure 7A and Supplementary Table S7). Particularly, Prw1, a component of the Clr6 complex I, achieves the highest percentage of sequence coverage identified from our MS data. In addition, we found that Rbm10 is copurified with Asf1/Cia1 and the HIRA histone chaperone complex. It has been shown that Asf1 interacts with HIRA to mediate heterochromatin silencing (44,45). We also found that Rbm10 associates with FACT, Spt6 and CHD1/Hrp3 chromatin remodelers. These chromatin remodeling factors have also been shown to be important for heterochromatin formation (46-48). We detected a strong link of Rbm10 with RSC, SWI/SNF, and Ino80 chromatin remodeling complexes. All thirteen members of the RSC complex and eleven of twelve members of the SWI/SNF complex were found in the MS results (Figure 7A and Supplementary Table S7). We also found that condensin components in the Rbm10-purified product. Condensin has been implicated in pericentromeric

heterochromatin assembly in fission yeast (10,49). In addition, Rbm10 interacts with Uhp1, an ubiquitinated histone-like protein, and Lsd2, a conserved histone demethylase, both of which are linked to heterochromatin formation (50,51). Rbm10 is also copurified together with Ccq1, which is required for silencing in telomere and facultative heterochromatin (52,53).

Notably, Rbm10 associates with transcription factors, including all five members of the PAF complex, and the transcriptional activator Byr3, which was detected with a sequence coverage of 65% and the highest intensity to mass ratio in the whole dataset. Heterochromatin in fission yeast can be transcribed during S phase of the cell cycle, and the non-coding transcripts are processed into siRNAs by RNAi machinery (10,14). These transcription factors may be involved in regulation of heterochromatin transcription.

Rbm10 interacts with splicing factors

Our MS analysis also detected more than 30 splicing factors interacting with Rbm10 (Table 1). Most of them are from the spliceosome A and B components, such as U1 snRNP, Sf3a and Sf3b, U2AF and NTC complex. This finding is in concordance with interaction data from human RBM10, which has been shown to be part of the spliceosome A and B complex (29-31). These results demonstrate that Rbm10 interaction with the spliceosome are conserved between human and fission yeast. Our data further indicate that, even though *rbm10* Δ mutant shows only modest changes in splicing, Rbm10 in fission yeast nevertheless is involved in RNA splicing, consistent with the Rbm10 overexpression data (Figure 3).

We note that all the TAP purification experiments were performed using cells expressing FLAG-HA-Rbm10 to a higher level than endogenous Rbm10. To rule out the possibility that

the interactions we identified are the artifacts caused by overexpression of Rbm10, we performed co-immunoprecipitation (co-IP) to validate the interactions of Prw1, a subunit of Clr6 complex, and Uaf2, a splicing factor, with Rbm10 under lowly-expressed condition. We coexpressed FLAG-HA-Rbm10 and one of the His-tagged prey proteins in the presence of 0.01 mM thiamine. Our co-IP experiments confirmed the interaction of Rbm10 with both Prw1 and Uaf2 (Figure 7B and C).

DISCUSSION

Previous studies have shown that human RBM10 is an RNA splicing protein, responsible for the X-linked TARP syndrome, although the mechanisms by which Rbm10 causes the disease remains unclear (24,25,27). In this study, we identified its homologue Rbm10 in fission yeast. We showed that Rbm10 in fission yeast interacts with a variety of splicing factors, and overexpression of Rbm10 results in strong intron retention. These data suggest that the role of Rbm10 in splicing regulation is conserved. Surprisingly, our genome-wide RNA analysis showed that deletion of *rbm10*⁺ in fission yeast results in minor splicing defects. However, heterochromatin formation is severely disrupted in *rbm10* mutant. Our data strongly support that abnormality in heterochromatin formation in the mutant arises independently from defects in splicing. We further demonstrated that Rbm10 interacts with heterochromatin factors, including Clr6 complex and chromatin remodelers, suggesting a novel mechanism underlying splicing factor-mediated heterochromatin silencing. Our findings reveal previously unrecognized features of Rbm10 in chromatin regulation, and may help elucidate its roles in human disease.

Role of Rbm10 in heterochromatin formation

As in mammals, heterochromatin in fission yeast is enriched with hypoacetylation of histones and H3K9 methylation. These heterochromatin hallmarks are instrumental for heterochromatin structure and function (1,3). In fission yeast, siRNAs generated from heterochromatin transcripts during S phase promotes H3K9me by guiding the ClrC complex containing the H3K9 methyltransferase, Clr4, to heterochromatin (10,11,14,54). It has been shown that splicing factors are required for RNAi-mediated heterochromatin assembly in fission yeast. However, the mechanism behind the role of splicing factors in heterochromatin assembly remains poorly understood. There is an ongoing discussion in the field as to whether splicing factors participate in heterochromatin formation directly. A study by Bayne *et al.* has shown that in splicing factor mutants, such as *prp10-1*, splicing and heterochromatin defects can be uncoupled. In addition, the heterochromatin defects in the *prp10-1* mutant cannot be rescued by expression of wild type RNAi genes, *ago1⁺* and *hrr1⁺*, which contain introns. They further found an RNAi component, Cid12, interacts with splicing factors, including Prp10. They proposed that splicing factors interact with the RNAi machinery to directly regulate RNAi-mediated heterochromatin silencing (21). However, a comprehensive analysis of global splicing changes in these studies were missing, leaving open the possibility that splicing changes of a yet unknown heterochromatin factor might be responsible for the heterochromatin defects. Indeed, the study by Kallgren *et al.* has shown that splicing factor mutants, such as *cwfl4*, result in the splicing defects in Ago1, which in turn lead to heterochromatin defects (23).

In this study, we performed the first comprehensive analysis on global splicing changes in a splicing mutant showing heterochromatin defects, which could potentially rule out any indirect influences. We show that deletion of *rbm10⁺* has little effect on splicing. In addition, Rbm10 interacts with a variety of heterochromatin factors, notably the HDAC Clr6 complex,

and chromatin remodeling HIRA, FACT, CHD1 and Spt6 components. These findings strongly suggest that Rbm10 is directly involved in heterochromatin formation. Rbm10-interacting splicing factor Cwf10 has been shown to be associated with pericentromeric transcripts (21). We propose that Rbm10 binds nascent heterochromatic transcripts, and serves as a platform to recruit the Clr6 complex and chromatin remodelers to heterochromatic region, which in turn promote heterochromatin assembly. Our study, together with previous findings, further suggests that different splicing subunits may play separate roles in regulation of heterochromatin formation.

Role of Rbm10 in regulation of RNA splicing

In addition to its role in heterochromatin formation, our data suggest conserved function of Rbm10 in splicing. We detected that a plethora of Rbm10-interacting partners in fission yeast are from spliceosomal A and B complexes, which recapitulate the known interactions of human RBM10. Furthermore, overexpression of Rbm10 in fission yeast leads to massive intron retention, which can be seen as an equivalent to human RBM10's function in promoting exon skipping in humans. These results suggest that fission yeast and human Rbm10 have retained similar function in RNA splicing.

However, we only observed the strong effect of Rbm10 on splicing in fission yeast when it is overexpressed. In the deletion mutant strain only very modest changes in splicing were detected, indicating a mild impact of Rbm10 on splicing at its endogenous expression level. We observed that Rbm10 expression level appears to be extremely low under normal cell growth condition. Given the fact that stoichiometric amounts of splicing factors are needed for splicing, our data indicate that Rbm10 does not serve as a general splicing factor under endogenous expression level. We speculate that higher expression of *rbm10*⁺ may be induced

under specific environmental conditions, leading to changes of gene expression through altering RNA splicing patterns. Due to its strong toxicity in overexpression, it is likely that *rbm10*⁺ expression level is tightly controlled and its dual function might be regulated dose-dependently.

Interactome of Rbm10

We show that Rbm10 interacts with around 850 proteins, with enrichment for splicing factors, HDAC, chromatin remodelers and transcription factors. These data strongly support the direct role of Rbm10 in heterochromatin formation and splicing. Both of these processes are involved with various large protein complexes, explaining the high number of interacting partners. Especially the good correlation between fission yeast and human RBM10 in regard to its interaction with the spliceosome can be seen as a proof-of-principle experiment.

Rbm10 interacts with transcription factors, especially Byr3, which has the highest sequence coverage of the whole dataset. Since heterochromatin formation is also dependent on transcription during S phase, we speculate that this factor may play a role in mediating heterochromatin transcription. Its exact role in heterochromatin regulation still needs further characterization in future studies. Interestingly, we also found that Rbm10 interacts with multiple replication factors (Figure 6D). Replication factors have also been implicated in heterochromatin and centromere assembly in fission yeast (14,55-58).

Comparison between fission yeast and human RBM10

The fact that Rbm10 interacts with the spliceosome and its overexpression results in intron retention indicates that the function of Rbm10 as a splicing factor is conserved between human and fission yeast. However, human RBM10 is expressed at substantially higher level

than fission yeast Rbm10. This may be due to the fact that human RBM10 regulates exon skipping that generates alternative spliced proteins, but fission yeast Rbm10, on the other hand, is mainly responsible for intron retention, which can lead to premature block of transcription and RNA degradation via nonsense-mediated RNA decay (NMD) pathway (59). Overexpression and knock-down of human RBM10 lead to massive changes in gene expression (24,25). Overexpression of human RBM10 also results in nuclear condensation (60). However, it is still not clear whether the defects are evoked by secondary effects, or result from that fact that human RBM10 has a role in heterochromatin formation and gene silencing. Nevertheless, human RBM10 was found to be part of H2A deubiquitinases complex (34), which has been implicated in heterochromatin regulation (61). Future work is needed to elucidate whether human RBM10 has a dual function in the regulation of splicing and heterochromatin formation.

DATA ACCESS

All genomic data were available at the GEO database under the accession number GSE93906.

SUPPLEMENTARY DATA

Supplementary Data are available Online.

FUNDING

This work was supported by National Institute of Health [R01 GM106037 to F.L.]; and National Science Foundation [MCB-1330557 to F.L.]. F. L. is a Pew Scholar in the Biomedical Sciences, supported by The Pew Charitable Trusts.

Conflict of interest statement. None declared.

ACKNOWLEDGMENTS

We thank Qianhua Dong and Jinpu Yang for critical reading of the manuscript.

REFERENCES:

1. Martienssen, R. and Moazed, D. (2015) RNAi and heterochromatin assembly. *Cold Spring Harb Perspect Biol*, **7**, a019323.
2. Elgin, S.C. and Reuter, G. (2013) Position-effect variegation, heterochromatin formation, and gene silencing in *Drosophila*. *Cold Spring Harb Perspect Biol*, **5**, a017780.
3. Wang, J., Jia, S.T. and Jia, S. (2016) New Insights into the Regulation of Heterochromatin. *Trends Genet*, **32**, 284-294.
4. Li, F., Goto, D.B., Zaratiegui, M., Tang, X., Martienssen, R. and Cande, W.Z. (2005) Two novel proteins, Dos1 and Dos2, interact with Rik1 to regulate heterochromatic RNA interference and histone modification. *Current Biology*, **15**, 1448-1457.
5. Horn, P.J., Bastie, J.N. and Peterson, C.L. (2005) A Rik1-associated, cullin-dependent E3 ubiquitin ligase is essential for heterochromatin formation. *Genes & Development*, **19**, 1705-1714.
6. Jia, S., Kobayashi, R. and Grewal, S.I. (2005) Ubiquitin ligase component Cul4 associates with Clr4 histone methyltransferase to assemble heterochromatin. *Nat Cell Biol*, **7**, 1007-1013.
7. Thon, G., Hansen, K.R., Altes, S.P., Sidhu, D., Singh, G., Verhein-Hansen, J., Bonaduce, M.J. and Klart, A.J.S. (2005) The Clr7 and Clr8 directionality factors and the Pcu4 cullin mediate heterochromatin formation in the fission yeast *Schizosaccharomyces pombe*. *Genetics*, **171**, 1583-1595.

8. Hong, E.J., Villen, J., Gerace, E.L., Gygi, S.P. and Moazed, D. (2005) A cullin E3 ubiquitin ligase complex associates with Rik1 and the Clr4 histone H3-K9 methyltransferase and is required for RNAi-mediated heterochromatin formation. *RNA Biol*, **2**, 106-111.
9. Li, F., Huarte, M., Zaratiegui, M., Vaughn, M.W., Shi, Y., Martienssen, R. and Cande, W.Z. (2008) Lid2 Is Required for Coordinating H3K4 and H3K9 Methylation of Heterochromatin and Euchromatin. *Cell*, **135**, 272-283.
10. Chen, E.S., Zhang, K., Nicolas, E., Cam, H.P., Zofall, M. and Grewal, S.I.S. (2008) Cell cycle control of centromeric repeat transcription and heterochromatin assembly. *Nature*, **451**, 734-737.
11. Kloc, A., Zaratiegui, M., Nora, E. and Martienssen, R. (2008) RNA interference guides histone modification during the S phase of chromosomal replication. *Current Biology*, **18**, 490-495.
12. Verdel, A., Jia, S., Gerber, S., Sugiyama, T., Gygi, S., Grewal, S.I. and Moazed, D. (2004) RNAi-mediated targeting of heterochromatin by the RITS complex. *Science*, **303**, 672-676.
13. Motamedi, M.R., Verdel, A., Colmenares, S.U., Gerber, S.A., Gygi, S.P. and Moazed, D. (2004) Two RNAi complexes, RITS and RDRC, physically interact and localize to noncoding centromeric RNAs. *Cell*, **119**, 789-802.
14. Li, F., Martienssen, R. and Cande, W.Z. (2011) Coordination of DNA replication and histone modification by the Rik1-Dos2 complex. *Nature*, **475**, 244-248.
15. Zaratiegui, M., Castel, S.E., Irvine, D.V., Kloc, A., Ren, J., Li, F., de Castro, E., Marin, L., Chang, A.Y., Goto, D. *et al.* (2011) RNAi promotes heterochromatic silencing through replication-coupled release of RNA Pol II. *Nature*, **479**, 135-138.

16. Gonzalez, M. and Li, F. (2012) DNA replication, RNAi and epigenetic inheritance. *Epigenetics*, **7**, 14-19.
17. Bjerling, P., Silverstein, R.A., Thon, G., Caudy, A., Grewal, S. and Ekwall, K. (2002) Functional divergence between histone deacetylases in fission yeast by distinct cellular localization and in vivo specificity. *Mol Cell Biol*, **22**, 2170-2181.
18. Nicolas, E., Yamada, T., Cam, H.P., Fitzgerald, P.C., Kobayashi, R. and Grewal, S.I. (2007) Distinct roles of HDAC complexes in promoter silencing, antisense suppression and DNA damage protection. *Nat Struct Mol Biol*, **14**, 372-380.
19. Shankaranarayana, G.D., Motamedi, M.R., Moazed, D. and Grewal, S.I. (2003) Sir2 regulates histone H3 lysine 9 methylation and heterochromatin assembly in fission yeast. *Curr Biol*, **13**, 1240-1246.
20. Buscaino, A., Lejeune, E., Audergon, P., Hamilton, G., Pidoux, A. and Allshire, R.C. (2013) Distinct roles for Sir2 and RNAi in centromeric heterochromatin nucleation, spreading and maintenance. *The EMBO journal*, **32**, 1250-1264.
21. Bayne, E.H., Portoso, M., Kagansky, A., Kos-Braun, I.C., Urano, T., Ekwall, K., Alves, F., Rappsilber, J. and Allshire, R.C. (2008) Splicing factors facilitate RNAi-directed silencing in fission yeast. *Science*, **322**, 602-606.
22. Chinen, M., Morita, M., Fukumura, K. and Tani, T. (2010) Involvement of the spliceosomal U4 small nuclear RNA in heterochromatic gene silencing at fission yeast centromeres. *The Journal of biological chemistry*, **285**, 5630-5638.
23. Kallgren, S.P., Andrews, S., Tadeo, X., Hou, H., Moresco, J.J., Tu, P.G., Yates, J.R., 3rd, Nagy, P.L. and Jia, S. (2014) The proper splicing of RNAi factors is critical for pericentric heterochromatin assembly in fission yeast. *PLoS Genet*, **10**, e1004334.
24. Wang, Y., Gogol-Doring, A., Hu, H., Frohler, S., Ma, Y., Jens, M., Maaskola, J., Murakawa, Y., Quedenau, C., Landthaler, M. *et al.* (2013) Integrative analysis

- revealed the molecular mechanism underlying RBM10-mediated splicing regulation. *EMBO molecular medicine*, **5**, 1431-1442.
25. Bechara, E.G., Sebestyen, E., Bernardis, I., Eyraas, E. and Valcarcel, J. (2013) RBM5, 6, and 10 differentially regulate NUMB alternative splicing to control cancer cell proliferation. *Molecular cell*, **52**, 720-733.
 26. Rodor, J., FitzPatrick, D.R., Eyraas, E. and Caceres, J.F. (2016) The RNA-binding landscape of RBM10 and its role in alternative splicing regulation in models of mouse early development. *RNA biology*, 1-13.
 27. Hernandez, J., Bechara, E., Schlesinger, D., Delgado, J., Serrano, L. and Valcarcel, J. (2016) Tumor suppressor properties of the splicing regulatory factor RBM10. *RNA biology*, **13**, 466-472.
 28. Matera, A.G. and Wang, Z. (2014) A day in the life of the spliceosome. *Nature reviews. Molecular cell biology*, **15**, 108-121.
 29. Rappsilber, J., Ryder, U., Lamond, A.I. and Mann, M. (2002) Large-scale proteomic analysis of the human spliceosome. *Genome research*, **12**, 1231-1245.
 30. Agafonov, D.E., Deckert, J., Wolf, E., Odenwalder, P., Bessonov, S., Will, C.L., Urlaub, H. and Luhrmann, R. (2011) Semiquantitative proteomic analysis of the human spliceosome via a novel two-dimensional gel electrophoresis method. *Molecular and cellular biology*, **31**, 2667-2682.
 31. Behzadnia, N., Golas, M.M., Hartmuth, K., Sander, B., Kastner, B., Deckert, J., Dube, P., Will, C.L., Urlaub, H., Stark, H. *et al.* (2007) Composition and three-dimensional EM structure of double affinity-purified, human prespliceosomal A complexes. *The EMBO journal*, **26**, 1737-1748.

32. Bessonov, S., Anokhina, M., Will, C.L., Urlaub, H. and Luhrmann, R. (2008) Isolation of an active step I spliceosome and composition of its RNP core. *Nature*, **452**, 846-850.
33. Hegele, A., Kamburov, A., Grossmann, A., Sourlis, C., Wowro, S., Weimann, M., Will, C.L., Pena, V., Luhrmann, R. and Stelzl, U. (2012) Dynamic protein-protein interaction wiring of the human spliceosome. *Molecular cell*, **45**, 567-580.
34. Zhu, P., Zhou, W., Wang, J., Puc, J., Ohgi, K.A., Erdjument-Bromage, H., Tempst, P., Glass, C.K. and Rosenfeld, M.G. (2007) A histone H2A deubiquitinase complex coordinating histone acetylation and H1 dissociation in transcriptional regulation. *Molecular cell*, **27**, 609-621.
35. Moreno, S., Klar, A. and Nurse, P. (1991) Molecular genetic analysis of fission yeast *Schizosaccharomyces pombe*. *Methods Enzymol*, **194**, 795-823.
36. Trapnell, C., Pachter, L. and Salzberg, S.L. (2009) TopHat: discovering splice junctions with RNA-Seq. *Bioinformatics*, **25**, 1105-1111.
37. Anders, S. and Huber, W. (2010) Differential expression analysis for sequence count data. *Genome Biol*, **11**, R106.
38. Laity, J.H., Lee, B.M. and Wright, P.E. (2001) Zinc finger proteins: new insights into structural and functional diversity. *Current opinion in structural biology*, **11**, 39-46.
39. Brown, R.S. (2005) Zinc finger proteins: getting a grip on RNA. *Current opinion in structural biology*, **15**, 94-98.
40. Lunde, B.M., Moore, C. and Varani, G. (2007) RNA-binding proteins: modular design for efficient function. *Nature reviews. Molecular cell biology*, **8**, 479-490.
41. Rhind, N., Chen, Z., Yassour, M., Thompson, D.A., Haas, B.J., Habib, N., Wapinski, I., Roy, S., Lin, M.F., Heiman, D.I. *et al.* (2011) Comparative functional genomics of the fission yeasts. *Science*, **332**, 930-936.

42. Wang, Y., Gogol-Doring, A., Hu, H., Frohler, S., Ma, Y., Jens, M., Maaskola, J., Murakawa, Y., Quedenau, C., Landthaler, M. *et al.* (2013) Integrative analysis revealed the molecular mechanism underlying RBM10-mediated splicing regulation. *EMBO Mol Med*, **5**, 1431-1442.
43. Manolis, K.G., Nimmo, E.R., Hartsuiker, E., Carr, A.M., Jeggo, P.A. and Allshire, R.C. (2001) Novel functional requirements for non-homologous DNA end joining in *Schizosaccharomyces pombe*. *The EMBO journal*, **20**, 210-221.
44. Greenall, A., Williams, E.S., Martin, K.A., Palmer, J.M., Gray, J., Liu, C. and Whitehall, S.K. (2006) Hip3 interacts with the HIRA proteins Hip1 and Slm9 and is required for transcriptional silencing and accurate chromosome segregation. *The Journal of biological chemistry*, **281**, 8732-8739.
45. Yamane, K., Mizuguchi, T., Cui, B., Zofall, M., Noma, K. and Grewal, S.I. (2011) Asf1/HIRA facilitate global histone deacetylation and associate with HP1 to promote nucleosome occupancy at heterochromatic loci. *Molecular cell*, **41**, 56-66.
46. Lejeune, E., Bortfeld, M., White, S.A., Pidoux, A.L., Ekwall, K., Allshire, R.C. and Ladurner, A.G. (2007) The chromatin-remodeling factor FACT contributes to centromeric heterochromatin independently of RNAi. *Current Biology*, **17**, 1219-1224.
47. Kiely, C.M., Marguerat, S., Garcia, J.F., Madhani, H.D., Bahler, J. and Winston, F. (2011) Spt6 is required for heterochromatic silencing in the fission yeast *Schizosaccharomyces pombe*. *Molecular and cellular biology*, **31**, 4193-4204.
48. Jae Yoo, E., Kyu Jang, Y., Ae Lee, M., Bjerling, P., Bum Kim, J., Ekwall, K., Hyun Seong, R. and Dai Park, S. (2002) Hrp3, a chromodomain helicase/ATPase DNA binding protein, is required for heterochromatin silencing in fission yeast. *Biochem Biophys Res Commun*, **295**, 970-974.

49. He, H., Zhang, S., Wang, D., Hochwagen, A. and Li, F. (2016) Condensin Promotes Position Effects within Tandem DNA Repeats via the RITS Complex. *Cell reports*, **14**, 1018-1024.
50. Naresh, A., Saini, S. and Singh, J. (2003) Identification of Uhp1, a ubiquitinated histone-like protein, as a target/mediator of Rhp6 in mating-type silencing in fission yeast. *The Journal of biological chemistry*, **278**, 9185-9194.
51. Lan, F., Zariatogui, M., Villen, J., Vaughn, M.W., Verdel, A., Huarte, M., Shi, Y., Gygi, S.P., Moazed, D. and Martienssen, R.A. (2007) S. pombe LSD1 homologs regulate heterochromatin propagation and euchromatic gene transcription. *Mol Cell*, **26**, 89-101.
52. Wang, J., Cohen, A.L., Letian, A., Tadeo, X., Moresco, J.J., Liu, J., Yates, J.R., 3rd, Qiao, F. and Jia, S. (2016) The proper connection between shelterin components is required for telomeric heterochromatin assembly. *Genes & development*, **30**, 827-839.
53. Zofall, M., Smith, D.R., Mizuguchi, T., Dhakshnamoorthy, J. and Grewal, S.I. (2016) Taz1-Shelterin Promotes Facultative Heterochromatin Assembly at Chromosome-Internal Sites Containing Late Replication Origins. *Mol Cell*, **62**, 862-874.
54. Yang, J. and Li, F. (2016) Are all repeats created equal? Understanding DNA repeats at an individual level. *Curr Genet*.
55. He, H., Gonzalez, M., Zhang, F. and Li, F. (2014) DNA replication components as regulators of epigenetic inheritance--lesson from fission yeast centromere. *Protein Cell*, **5**, 411-419.
56. Nakayama, J., Allshire, R.C., Klar, A.J.S. and Grewal, S.I.S. (2001) Role for DNA polymerase alpha in epigenetic control of transcriptional silencing in fission yeast. *Embo Journal*, **20**, 2857-2866.

57. Natsume, T., Tsutsui, Y., Sutani, T., Dunleavy, E.M., Pidoux, A.L., Iwasaki, H., Shirahige, K., Allshire, R.C. and Yamao, F. (2008) A DNA Polymerase alpha Accessory Protein, Mc11, Is Required for Propagation of Centromere Structures in Fission Yeast. *Plos One*, **3**, 14.
58. Gonzalez, M., He, H., Sun, S., Li, C. and Li, F. (2013) Cell cycle-dependent deposition of CENP-A requires the Dos1/2-Cdc20 complex. *Proc Natl Acad Sci U S A*, **110**, 606-611.
59. Lejeune, F. and Maquat, L.E. (2005) Mechanistic links between nonsense-mediated mRNA decay and pre-mRNA splicing in mammalian cells. *Current opinion in cell biology*, **17**, 309-315.
60. Wang, K., Bacon, M.L., Tessier, J.J., Rintala-Maki, N.D., Tang, V. and Sutherland, L.C. (2012) RBM10 Modulates Apoptosis and Influences TNF-alpha Gene Expression. *Journal of cell death*, **5**, 1-19.
61. Braun, S. and Madhani, H.D. (2012) Shaping the landscape: mechanistic consequences of ubiquitin modification of chromatin. *EMBO reports*, **13**, 619-630.

FIGURES

Figure 1. Human RBM10 is conserved in *S. pombe*. **(A)** Schematic diagram showing the domain structure of Rbm10 in *S. pombe*. **(B)** Rbm10 is enriched in the nucleus. Rbm10-GFP was constructed at its native locus under the control of its own promoter.

Figure 2. Overexpression of Rbm10 results in severe growth defects and massive intron retention. **(A)** Cells overexpressing Rbm10 display slow growth. Serial dilutions of indicated cells carrying pREP1-*rbm10* were plated in minimal medium without thiamine. Empty pREP1 vector was used as a control. Ctrl, a control plate containing thiamine. **(B)** Cells overexpressing Rbm10 showed abnormal cell shapes and nuclear organization. Left, bright-field microscopic images. Right, DAPI staining. OE, overexpression. **(C)** MA plot comparing the intron retention patterns between *rbm10*-overexpressing cells and WT. Log₂ transformed read count for each event was plotted on the X axis, and the PIR difference was on the Y axis. The red and blue dots represented the events with significantly different intron retention patterns. The grey lines indicate 10% PIR difference.

Figure 3. Deletion of Rbm10 has minor effect on gene expression and intron retention. **(A)** MA plot comparing the gene expression patterns between *rbm10*Δ cells and WT. The average read count for each gene was plotted on the X axis, and the log₂ transformed fold change was on the Y axis. The red and blue dots represented the genes with significantly different gene expression patterns. **(B)** MA plot comparing the intron retention patterns between *rbm10*Δ cells and WT. Log₂ transformed read count for each event was plotted on the X axis, and the PIR difference was on the Y axis. The red and blue dots represented the events with significantly different intron retention patterns. The grey lines indicate 10% PIR difference. **(C)** MA plot comparing the exon skipping patterns between *rbm10*Δ cells and WT. Log₂ transformed read count for each event was plotted on the X axis, and the Percent Spliced In difference (ΔPSI) was on the Y axis. The red dots represented the events with significantly different exon skipping patterns. The grey lines indicate 10% PIR difference.

Figure 4. Rbm10 is important for heterochromatin silencing. **(A)** Serial dilutions of indicated cells harboring *ura4*⁺ at the *otr* region were plated in minimal medium without uracil (-Ura) or with the counter-selective FOA media. Ctrl, a control plate containing uracil. WT, wild type. **(B)** Serial dilutions of *rbm10*Δ cells and WT as control carrying *his3*⁺ at the telomeric region (*tel*) were plated in minimal medium without histidine (-His). **(C)** Growth assays of *rbm10*Δ and WT cells carrying *ura4*⁺ at the mating-type region in medium without uracil (-Ura) or with the FOA media. **(D)** Analysis of H3K9 methylation in the *otr* region by ChIP. ChIP assays were performed using an antibody against H3K9 methylation and primers specific for in the *otr* region. Representative results are shown. *act1*⁺ was used as a control.

Figure 5. Silencing defects do not result from mis-splicing of heterochromatin factors. **(A)** Schematics of the exon-intron structure of *pku70*⁺. *pku70*⁺ has six introns (1 to 6). Dark boxes indicate exons, connecting lines indicate introns, and white boxes represent untranslated regions (UTRs). **(B)** Barplot comparing the intron retention patterns between *rbm10*Δ mutant and WT for different introns of *pku70*⁺. Intron retention was analyzed by RT-PCR. **(C)** Expression of *pku70*⁺ was unable to rescue the heterochromatin defect in *rbm10*Δ mutant. Serial dilutions of indicated cells harboring *his3*⁺ at the telomeric region were plated in minimal medium without histidine (-His) and thiamine. Empty pREP1 vector was used as a control. Ctrl, a control plate containing histidine.

Figure 6. Mass spectrometry analysis of TAP-tag purified Rbm10. **(A)** Cells carrying FLAG-HA tagged Rbm10 under its own promoter expressed from its endogenous locus display no detectable silencing defect. Serial dilutions of indicated cells harboring *ura4*⁺ at the *otr* region were plated in minimal medium containing FOA. Ctrl, a control plate without FOA. **(B)** A silver-stained gel showing the TAP-tag purification of Rbm10 and a control

purification from an untagged strain. **(C)** Venn diagram showing the overlap of proteins detected by mass spectrometry. **(D)** The proteins identified by mass spectrometry were grouped based on their functions, as indicated in the table.

Figure 7. Rbm10 interacts with factors involved in heterochromatin formation and splicing.

(A) Components of HDAC Clr6 and chromatin remodeling complexes identified by mass spectrometry analysis of Rbm10 were listed. Condensin components and other known heterochromatin factors identified were also shown. **(B)** Cell lysates from cells expressing Prw1-FLAG-His and FLAG-HA- Rbm10 at low level in the presence of 0.01 mM thiamine were subjected to immunoprecipitation with uMACS HA magnetic beads. Cells expressing Prw1-FLAG-His alone was used as a control. Precipitated proteins were analyzed by Western blotting using indicated antibodies. **(C)** Cell lysates from cells expressing low level of Uaf2-FLAG-His and FLAG-HA-Rbm10 were subjected to immunoprecipitation with uMACS HA magnetic beads, and analyzed by Western blotting using indicated antibodies. Cells expressing Uaf2- FLAG-His only was used as a control.

Figure 1

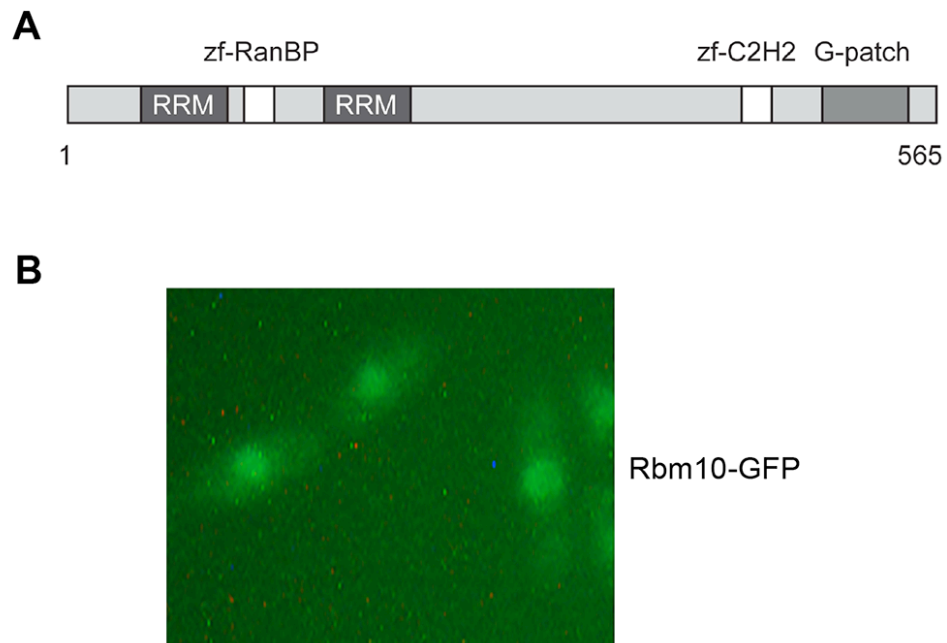


Figure 2

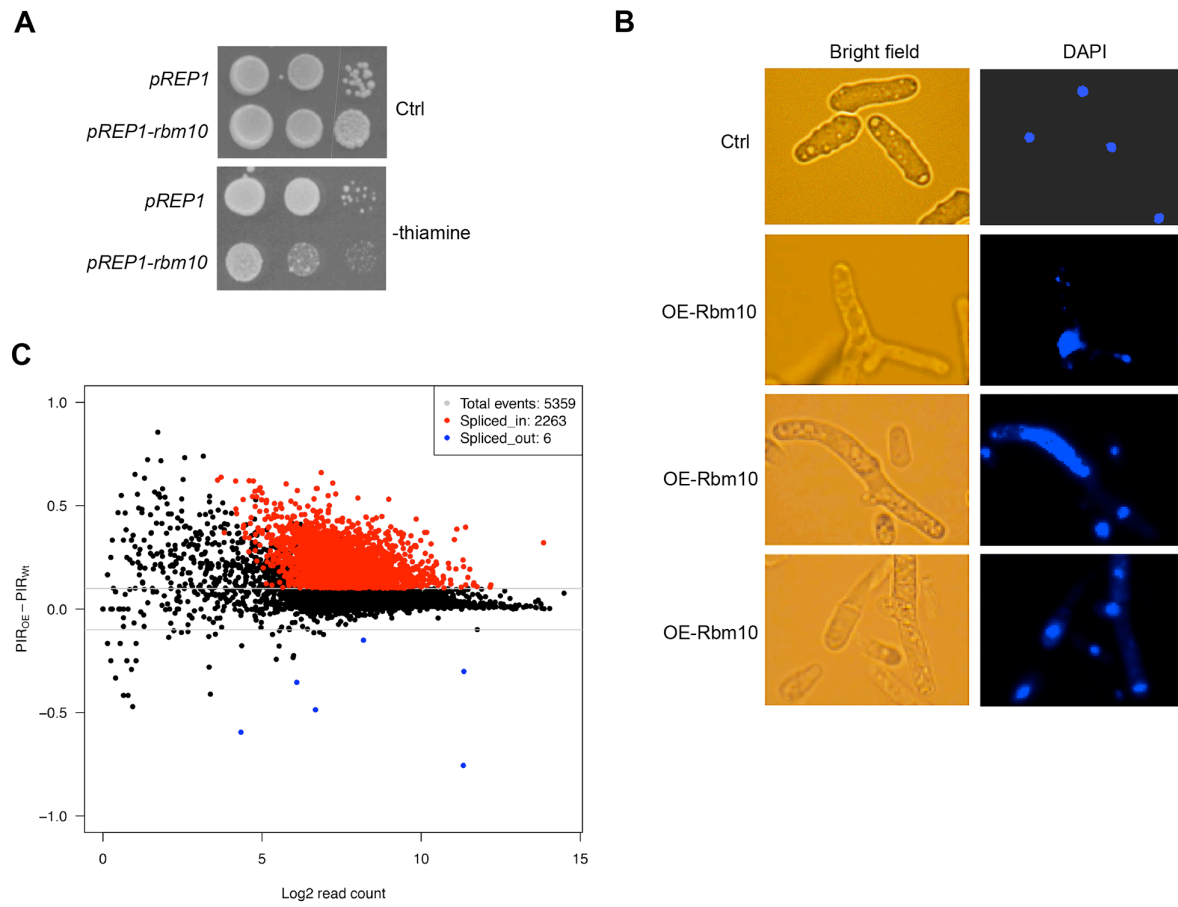


Figure 3

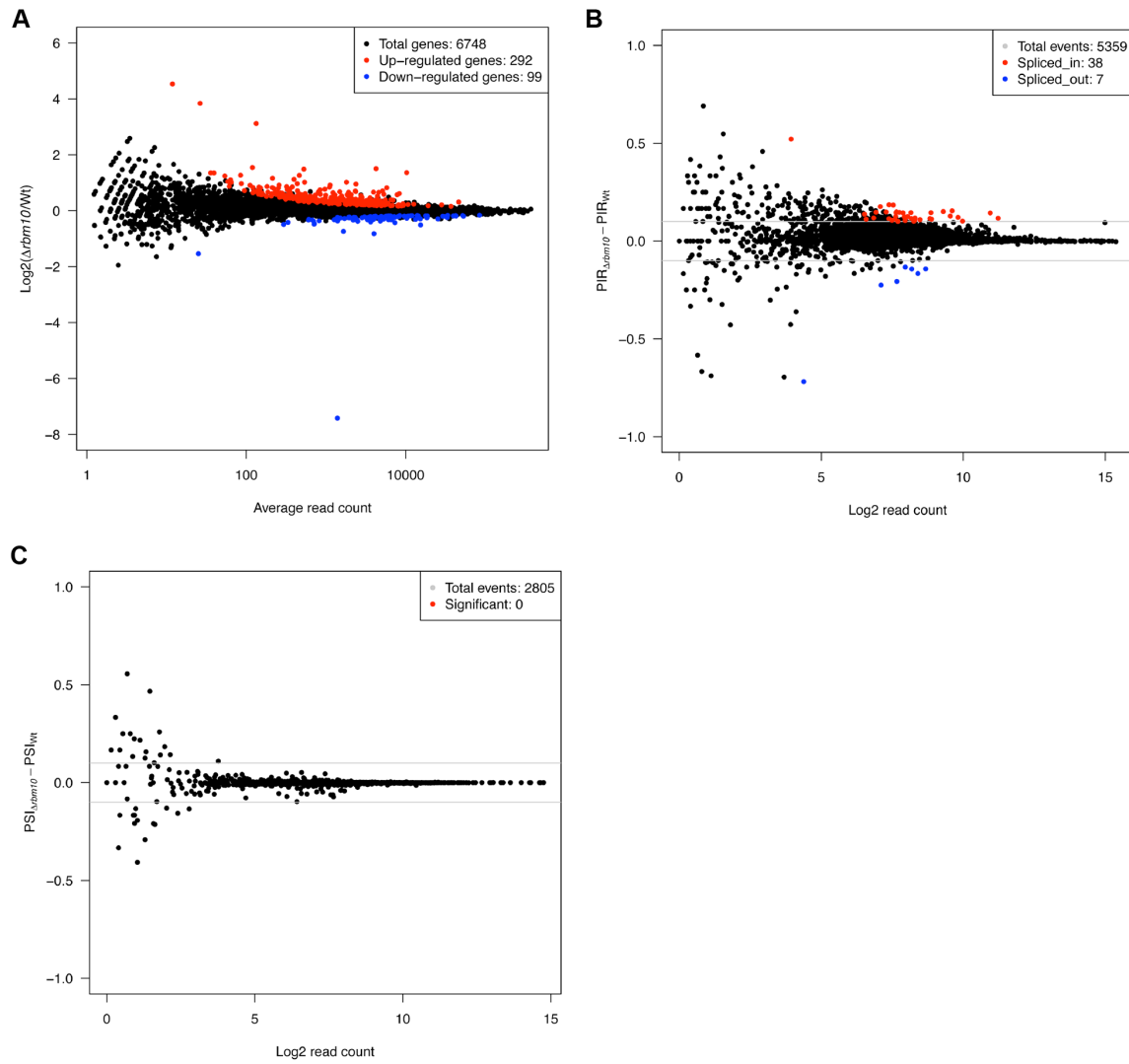


Figure 4

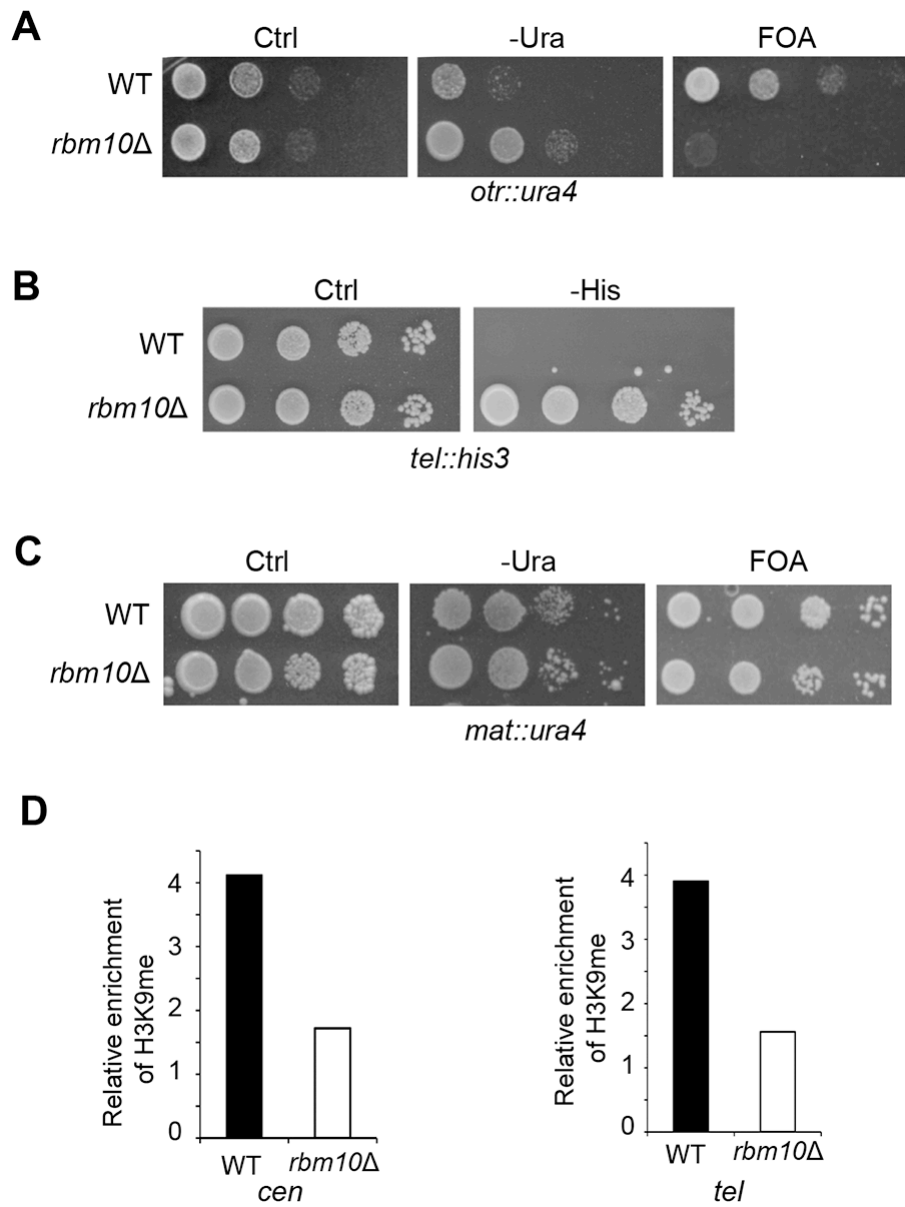


Figure 5

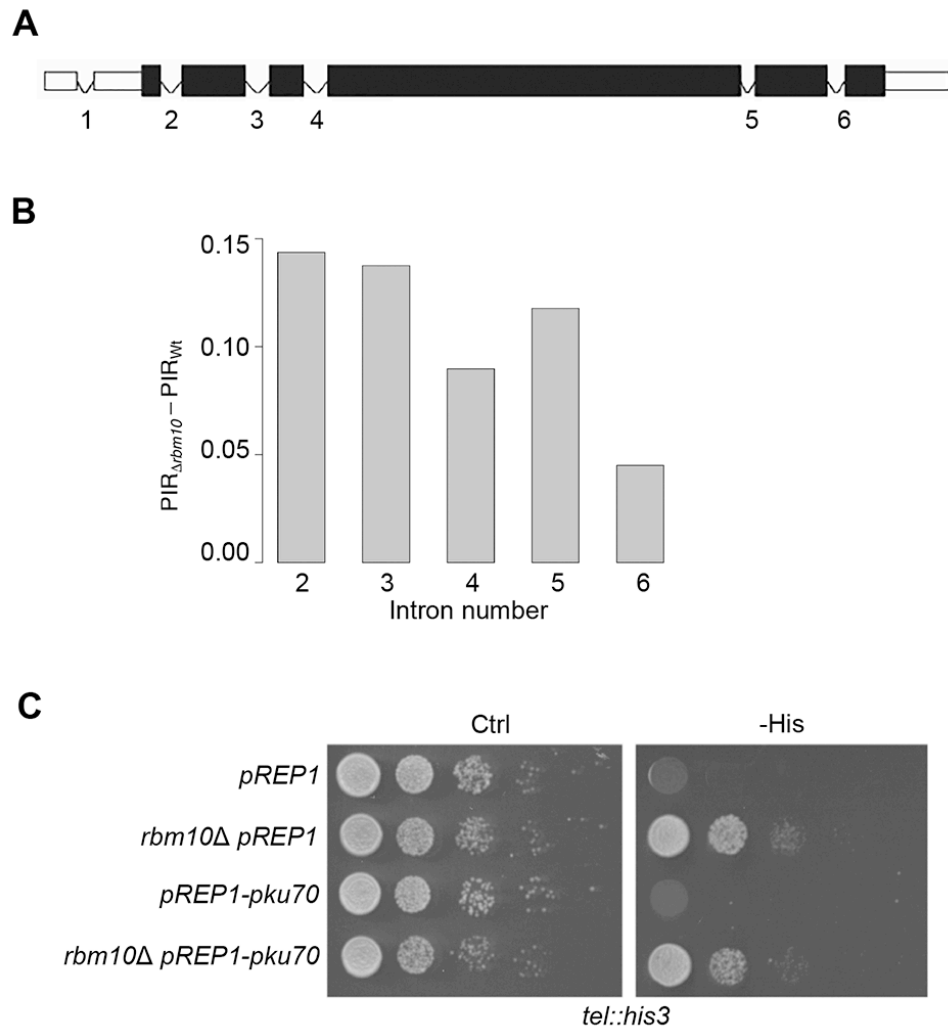


Figure 6

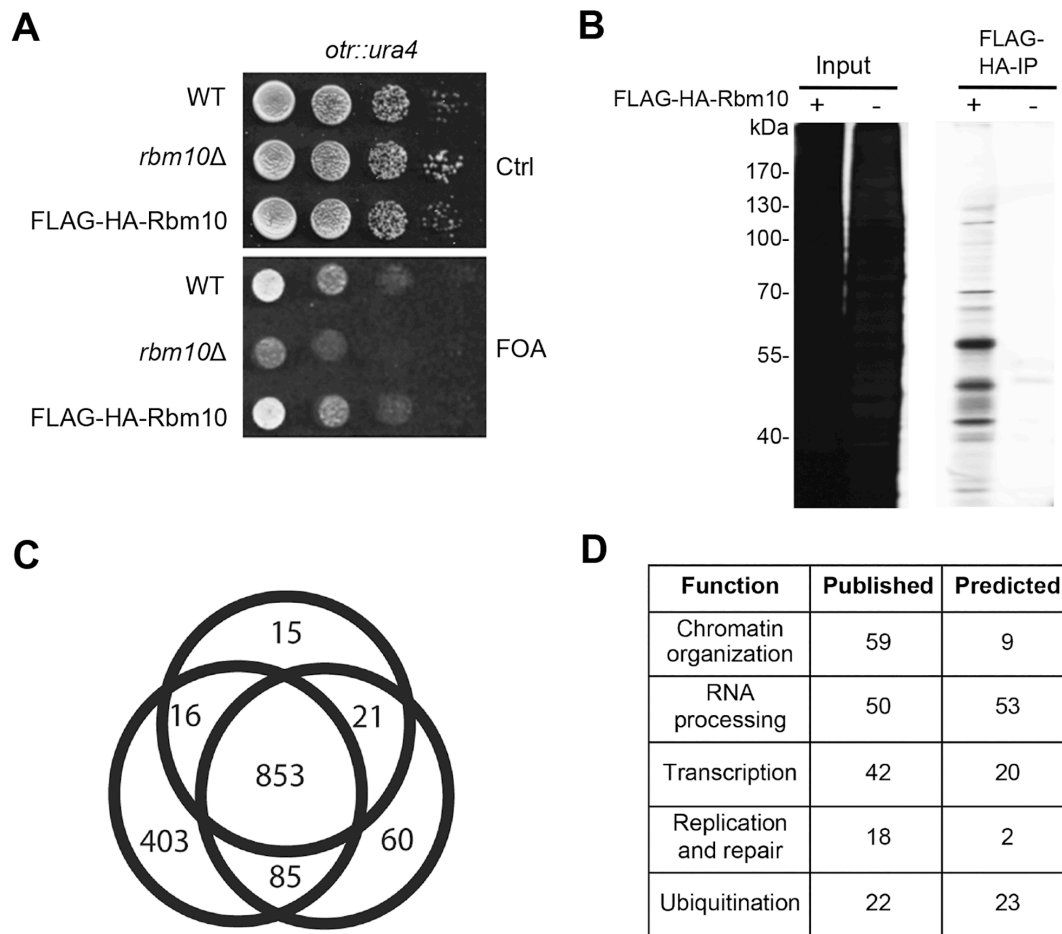
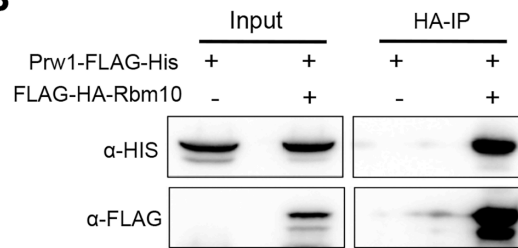


Figure 7

A

Clr6	Alp13, Clr6, Prw1, Pst1, Rxt3, Sds3
Asf1/HIRA	Cia1, Hip1, Slm9
FACT	Spt16
Ino80	Alp5, Arp5, Arp42, les2, les4, Ino80
SWI/SNF	Sol1, Arp8, Arp9, Arp42, Ssr1, Ssr2, Ssr3, Ssr4, Snf5, Snf22, Snf30
RSC	Arp42, Arp9, Rsc7, Rsc58, Rsc1, Rsc4, Rsc9, Sfh1, Ssr1, Ssr2, Ssr3, Ssr4, Snf21
CHD1	Hrp3
Spt6	Spt6
Condensin	Cnd2, Cut14
Others	Ccq1, Lsd2

B



C

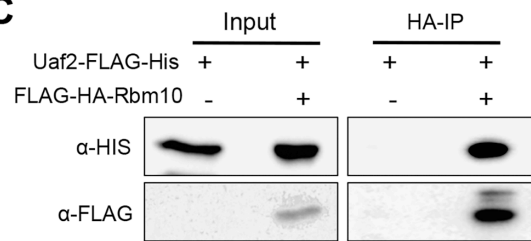


Table 1. Splicing factors that Rbm10 interacts with

ID	Name	Description
SPAC4D7.13	Usp104	U1 snRNP-associated protein Usp104
SPBC4B4.09	Usp105	U1 snRNP-associated protein Usp105
SPBC839.10	Usp107	U1 snRNP-associated protein Usp107
SPAP8A3.06	Uaf2	U2AF small subunit, U2AF-23
SPAC9.03c	Brr2	U5 snRNP complex subunit Brr2
SPAC644.12	Cdc5	cell division control protein, splicing factor Cdc5
SPBC19C2.01	Cdc28	ATP-dependent RNA helicase Prp8
SPBC16A3.18	Cip1	RNA-binding protein Cip1
SPBC215.12	Cwf10	U5 snRNP GTPase subunit Cwf10
SPCP1E11.07c	Cwf18	complexed with Cdc5 protein Cwf18
SPAC3A12.11c	Cwf2	RNA-binding protein Cwf2
SPBC211.02c	Cwf3	complexed with Cdc5 protein Cwf3
SPBC31F10.11c	Cwf4	complexed with Cdc5 protein Cwf4
SPCC550.02c	Cwf5	RNA-binding protein Cwf5
SPBC354.12	Gpd3	glyceraldehyde 3-phosphate dehydrogenase Gpd3
SPBC29A10.10c	Db18	tRNA-splicing endonuclease positive effector Db18
SPAC23H3.02c	Ini1	RING finger-like protein Ini1
SPBC6B1.07	Prp1	U4/U6 x U5 tri-snRNP complex subunit Prp1
SPAC27F1.09c	Prp10	U2 snRNP-associated protein Sap155
SPCC10H11.01	Prp11	ATP-dependent RNA helicase Prp11
SPAPJ698.03c	Prp12	U2 snRNP-associated protein Sap130
SPAC29A4.08c	Prp19	ubiquitin-protein ligase E4
SPBC1861.04c	Prp24	RNA-binding protein Prp24 (predicted)
SPBC119.13c	Prp31	U4/U6 x U5 tri-snRNP complex subunit Prp31
SPBC16H5.10c	Prp43	ATP-dependent RNA helicase Prp43
SPBP22H7.07	Prp5	WD repeat protein Prp5
SPAC227.12	Rna4	U4/U6 x U5 tri-snRNP complex subunit Prp4 family, Rna4
SPAC19G12.07c	Rsd1	RNA-binding protein Rsd1 (predicted)
SPAC22A12.09c	Sap114	U2 snRNP subunit Sap114
SPBC29A3.07c	Sap14	U2 snRNP-associated protein SF3B14 Sap14
SPAC22F8.10c	Sap145	U2 snRNP-associated protein Sap145
SPBC36.09	Sap61	U2 snRNP-associated protein sap61
SPAC4F8.12c	Spp42	U5 snRNP complex subunit Spp42
SPAC4D7.13	Usp104	U1 snRNP-associated protein Usp104
SPBC4B4.09	Usp105	U1 snRNP-associated protein Usp105
SPBC839.10	Usp107	U1 snRNP-associated protein Usp107